

Random Party Distillation on a Superconducting Processor

Alexander C.B. Greenwood,^{1,*} Jackson Russett,¹ Hoi-Kwong Lo,^{1,2,3} and Li Qian¹

¹*Dept of Electrical & Computer Engineering, University of Toronto
Toronto, Ontario, Canada M5S 3G4*

²*Department of Physics, National University of Singapore Blk S12 Level 2, 2 Science Drive 3 Singapore 117551*

³*Quantum Bridge Technologies Inc., 108 College Street, Toronto, Canada*

(Dated: August 13, 2025)

Random party distillation refers to the process by which Einstein-Podolsky-Rosen pairs are randomly extracted from a single copy of a multipartite entangled state after multiple rounds of performing positive operator value measure operations. In this work, we propose a qubit-based implementation of a random party distillation protocol and demonstrate its efficacy on the superconducting hardware device, `ibm_quebec`. We demonstrate a 4-round implementation of the protocol, showing distillation rates superior (~ 0.81 pairs/ W state) to the state of the art. Finally, we explore the dynamical properties of the protocol when implemented on superconducting hardware, and how errors introduced by mid-circuit measurements can be mitigated.

Entanglement is the essence of quantum mechanics [1]. The task of establishing bipartite correlations between physically distant parties is a basic subroutine necessary for quantum communications, particularly while teleporting qubits or gate operations. An active area of research is concerned with the distribution of entanglement between laboratories separated by hundreds of kilometers of optical fiber [2], or transmon qubits that are spaced hundreds of micrometers to millimeters apart [3, 4].

Random party distillation [5], is an interesting paradigm for studying multipartite entanglement and its conversion to bipartite entanglement. Unlike the bipartite case, multipartite entanglement lacks consensus of a “maximally-entangled” state, which depends on one’s choice of measure [6]. One may consider an operational approach to quantifying entanglement, such as a state’s capabilities of extracting bipartite entanglement, as in concentratable entanglement [7], entanglement of assistance [8, 9] or random party distillation, studied through the monotones introduced in [10, 11]. The latter of the three involves measuring a single copy of a multipartite entangled state in a higher-dimensional Hilbert space to probabilistically extract Einstein-Podolsky-Rosen (EPR) pairs over the course of many rounds of execution N . The probability of obtaining a single EPR pair from one copy of a W state converges to unity in the large limit $N \rightarrow \infty$. The main benefit of random party distillation is that it enables the distribution of bipartite entanglement to parties possessing a pre-shared multipartite entangled state. In spite of its proposed practical benefits, random party distillation has mainly been explored theoretically, finding applications in the first demonstration of a gap between separable (SEP) operations and local operations and classical communication (LOCC) [11], studying the complexity of round-trip LOCC [12] and improving resolution limits in long-baseline telescopy [13]. However, experimental implementations have been limited to single-round executions [14] and are therefore restricted

in achievable success probability.

In this letter, we present an experimental demonstration of random party distillation on the superconducting processor, `ibm_quebec`, that is capable of executing over four rounds of the protocol with a distillation rate of 0.81 pairs/ W state (superior to existing implementations). We introduce a generalized version of the protocol originally proposed by Fortescue and Lo [5], adapted for qubit systems without requiring access to higher energy levels. Creating multiparticle entanglement with transmon qubits and shielding it from dephasing is not an easy task; we show how the number of rounds of execution, and thus, success probability of our protocol, can be extended by means of dynamical decoupling and matrix-free measurement error mitigation (M3) [15].

We consider EPR distillation with three parties, although our method can be extended to larger multiparticle systems, using protocols described in [16, 17]. Alice, Bob, and Charlie wish to distill the triplet state:

$$|\Psi^+\rangle_{ij} = \frac{1}{\sqrt{2}} (|01\rangle + |10\rangle)_{ij} \quad \text{where } i, j \in \{a, b, c\} \text{ and } i \neq j, \quad (1)$$

from a W -class state of the form

$$|W\rangle_{abc} = \frac{1}{\sqrt{3}} (|011\rangle + |101\rangle + |110\rangle)_{abc}. \quad (2)$$

The simplest way for Alice, Bob, and Charlie to proceed is to specify one party to perform a strong measurement on their respective qubit in the Z basis. If the specified party measures a “1”, the other two parties will share an EPR pair. Measurement of a “0” indicates that the other parties share a product state. In this protocol, called *specific party distillation*, the probability of successful distillation $P(EPR) = 2/3$, from a single copy of a W state according to (2). If we wanted to increase the probability of a successful distillation event, we would

need to use a method that better leverages the shared entanglement of all three parties.

By allowing the randomness of which pair of parties ultimately share an EPR pair, one can increase the success rate. This *random party distillation* protocol, proposed by Fortescue and Lo [5], consists of each party coupling their qubit to a higher-dimensional Hilbert space, followed by a series of projective measurements to determine the presence of two-qubit entanglement while minimizing disturbance to the system itself. Later implementations such as [12] or [14] generalize the action of coupling to a higher-dimensional Hilbert space to a weak measurement process. Unlike projective (strong) measurements that completely destroy entanglement, weak measurements allow subsystems to remain entangled, albeit with less information extraction.

The objective of random party distillation is to increase the probability of extracting an EPR pair $P(EPR)$ to unity for a single *copy* of the W state in the asymptotic limit of LOCC operation rounds. This is a class of protocol where the probability of success is defined for a single copy of a W state reused over multiple rounds of protocol execution. It is important to note the contrast with “entanglement of assistance” [8], where one repeats a protocol over many identically prepared *copies* of a state until success.

In what follows, we describe the random distillation protocol on the superconducting hardware device, `ibm_quebec`. We detail the implementation of our random distillation protocol on `ibm_quebec` superconducting hardware and demonstrate how weak measurements can be realized on such hardware by introducing ancillary qubits coupled to the system of target qubits.

Suppose Alice, Bob, and Charlie start with a W -state of the form in (2). They apply the following operation to the state, coupling their respective qubits to the ancillae with an $0 < \epsilon \ll 1$:

$$\begin{aligned} |0\rangle_{A_i} |1\rangle_i &\rightarrow \sqrt{1-\epsilon^2} |0\rangle_{A_i} |1\rangle_i + \epsilon |1\rangle_{A_i} |1\rangle_i, \\ |0\rangle_{A_i} |0\rangle_i &\rightarrow |0\rangle_{A_i} |0\rangle_i, \end{aligned} \quad (3)$$

where i denotes the qubit in the W state (a, b, c) and A_i is for the corresponding ancilla (α, β, γ). Each ancilla starts in its ground state, $|0\rangle$, and ϵ represents the strength of the coupling measurement. After this operation, the parties possess the following state:

$$\begin{aligned} |W'\rangle &= (1 - \epsilon^2) |000\rangle_{\alpha\beta\gamma} |W\rangle_{abc} \\ &+ \epsilon \sqrt{\frac{2(1-\epsilon^2)}{3}} \left[|001\rangle_{\alpha\beta\gamma} |1\rangle_c |\Psi^+\rangle_{ab} \right. \\ &+ |010\rangle_{\alpha\beta\gamma} |1\rangle_b |\Psi^+\rangle_{ac} + |100\rangle_{\alpha\beta\gamma} |1\rangle_a |\Psi^+\rangle_{bc} \left. \right] \\ &+ O(\epsilon^2). \end{aligned} \quad (4)$$

Measurement outcome	Probability	Resulting state	Next step
$ 000\rangle_{\alpha\beta\gamma}$	$(1 - \epsilon^2)^2$	$ W\rangle_{abc}$	repeat
$ 100\rangle_{\alpha\beta\gamma}$	$\frac{2\epsilon^2(1-\epsilon^2)}{3}$	$ \Psi^+\rangle_{bc}$	exit - success
$ 010\rangle_{\alpha\beta\gamma}$	$\frac{2\epsilon^2(1-\epsilon^2)}{3}$	$ \Psi^+\rangle_{ac}$	exit - success
$ 001\rangle_{\alpha\beta\gamma}$	$\frac{2\epsilon^2(1-\epsilon^2)}{3}$	$ \Psi^+\rangle_{ab}$	exit - success
...	ϵ^4	N/A	exit - failure

TABLE I. Alice, Bob, and Charlie’s outcomes after each stage of weak measurements, and their respective probabilities of occurrence.

The three parties now each make a Z-basis measurement on their respective ancilla using the following projectors: $F = |0\rangle_{A_i} \langle 0|_{A_i}$ and $G = |1\rangle_{A_i} \langle 1|_{A_i}$. We can identify the possible outcomes of the three measurements based on the terms in (4). Measuring “0” corresponds to F and “1” to G . If two parties obtain an outcome of “0” and one party obtains an outcome of “1”, then the two parties that measured “0” possess an EPR pair among themselves. If two or more parties see an outcome of “1” then protocol ends immediately without distillation; the protocol fails. If all three parties obtain an outcome of “0”, then they possess a W state and the protocol repeats itself. All relevant results from the measurements of the ancillae are summarized in Table I.

After all N rounds are complete, an additional strong measurement step is added, unlike the original proposal in [18]. This is shown in Figure 1 where the final strong measurement is made on Alice’s qubit. This means that when all rounds of measurement end in a W -state, a final attempt remains with a $2/3$ probability of successfully obtaining an EPR state between Bob and Charlie. This additional step, as proposed in [14], helps increase the overall success probability when only a few rounds of measurements are accessible.

Weak measurements are performed on superconducting qubits using a controlled rotation gate, $CRY(\theta)$. Each round of the protocol consists of Alice, Bob, and Charlie applying the controlled rotation between their respective qubits and ancillae. A matrix representation of the $CRY(\theta)$ operation is given as follows:

$$CRY(\theta)_{A_i, i} = \mathbb{1} \otimes |0\rangle\langle 0| + RY(\theta) \otimes |1\rangle\langle 1| \quad (5)$$

The choice of θ is related to the measurement strength ϵ in Eq. (3) by $\theta = 2 \arcsin(\epsilon)$.

For simplicity, we assume that, in each round of the protocol, all three parties utilize the same value ϵ (which can be round-dependent). Thus, the same measurement strength, for their operations and choose ϵ to maximize

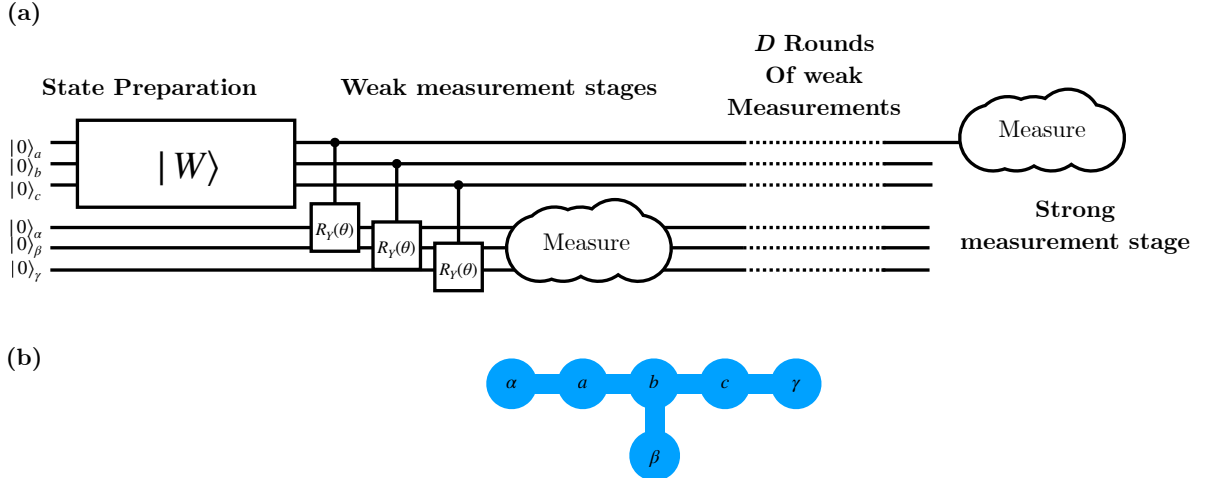


FIG. 1. (a) The circuit used to implement a D -round random party distillation protocol. Each controlled $R_y(\theta)$ operation facilitates the coupling between a single party’s qubit and its respective ancilla. A measurement on each parties ancillary qubit effectively corresponds to a weak measurement of the system qubits: a , b , and c . If after D rounds of measurements the protocol has not succeeded, one of the three parties (Alice) will perform a strong measurement on their qubit. (b) An illustration of the qubit connectivity required to implement the circuit in (a).

the probability of eventually distilling an EPR pair. For N rounds of measurements, the maximum success probability is

$$P_N = \frac{N+2}{N+3}, \quad (6)$$

when ϵ_D is optimized for each round as proposed in [14]. This accounts for all rounds of weak measurements and the final strong measurement to finish the protocol. The optimal choice of ϵ , as defined in [18] and improved in [14], is

$$\epsilon_D = \frac{1}{\sqrt{D+5}}. \quad (7)$$

The value of ϵ_D is determined by the number of *remaining* rounds, D , in the protocol. This means that each measurement round is stronger than the preceding round. Of course, Eqs. (6) and (7) assume that we began with an ideal W state, which is never the case on NISQ (near intermediate scale quantum) hardware. To this end, we shall now describe the characterization of the physical implementation and compare its performance to the theory.

Our random party distillation experiment was carried out on the 127-qubit system, `ibm_quebec`. The protocol outlined in this work is applicable to modalities of quantum computing outside of transmon qubits, i.e. trapped-ion, photonic, qubits, etc. However, the utility of random party distillation is observed particularly in instances where qubits have limited connectivity to one another and measurements take place on a timescale

much smaller than the coherence times of qubits. Fig. 1b shows an example of a connectivity graph between qubits on `ibm_quebec`, where edges between qubits indicate that an entanglement gate operation (in this case, an echoed cross-resonance gate) may be performed and the nodes represent qubits.

The protocol outlined in Fig. 1 requires *dynamic circuits*: circuits whose operations are determined by the results of its mid-circuit measurements [3]. In this case, the protocol only continues if Alice, Bob, and Charlie simultaneously measure a “0” bit during a round of weak mid-circuit measurements. This outcome indicates that a W -state is still present and that another round of weak measurements can be performed.

The following characterization steps: initial W -state fidelity, measurement of distillation rate, evolution of state fidelity, and entanglement of formation have all been considered using static circuits with mid-circuit measurement. Functionally, these circuits are nearly equivalent to the dynamic case, except that the success of distillation is determined after executing a predetermined number of rounds of execution rather than completing at the first detection of bipartite entanglement. An experimental challenge with mid-circuit measurements in IBM quantum computers is that the measurement time is rather long ($\sim 1\mu s$), during which idle qubits may decohere. To reduce errors due to decoherence during the mid-circuit measurement, it is important to apply error mitigation techniques such as dynamical decoupling. For information pertaining to the coherence and dephasing time of qubits used in this work, the reader is encouraged to consult the corresponding supplementary material.

After each round of Alice, Bob, and Charlie applying

$CRY(\theta)$ operations, the three parties make Z-basis measurements on their ancilla qubits. The probability of the protocol succeeding, two parties sharing an EPR pair can be expressed as

$$P_{\text{success}} = P_1(\text{EPR}) + \sum_{k=2}^N P_{k-1}(W)P_k(\text{EPR}|W) + P_s(\text{EPR}|W_N)P_N(W), \quad (8)$$

where $P_k(\text{EPR})$ and $P_k(W)$ correspond to the probabilities of obtaining an EPR pair and W state, respectively, in round k out of a total of N rounds. $P_s(\text{EPR}|W_N)$ corresponds to the probability of obtaining an EPR during the strong measurement stage given that a W state was detected during the final stage of weak measurements. These probabilities can be experimentally determined by preparing many copies of a W state, and repeating the execution of the protocol. By counting the number of instances in which all three parties measure “0” in a given round k , one can determine the probability of obtaining a W state. Likewise, by counting the number of instances in which one of the three parties measures “1”, the probability of successfully distilling an EPR pair may be obtained.

So far, we have considered an ideal implementation of random party distillation with perfect qubits and gate operations. Now we consider an imperfect scenario where the W state that we began with at each round of execution is not ideal and gate operations performed by Alice, Bob, and Charlie have non-unity fidelity. Consequently, the *expected* amount of bipartite entanglement $\langle E \rangle$ distilled from the protocol should be calculated by weighting each term in (8) by an entanglement measure $E(\rho_i^k)$ of the corresponding distilled pair:

$$\langle E \rangle = \frac{1}{|\mathcal{S}|} \sum_{i \in \mathcal{S}} P_1(\text{EPR})E(\rho_i^1) + \frac{1}{|\mathcal{S}|} \sum_{i \in \mathcal{S}} \sum_{k=2}^N P_{k-1}(W)P_k(\text{EPR}|W)E(\rho_i^k) + P_s(\text{EPR}|W_N)P_N(W)E(\rho_a^s) \quad (9)$$

where ρ_i^k is the bipartite state extracted in round k when the i th party measures an outcome of G during their respective projective measurement stage. We have denoted ρ_a^s as the distilled pair possessed by Bob and Charlie after successfully completing the final strong measurement stage. The set \mathcal{S} is defined as the set of parties involved in the protocol. For the purpose of this letter, $\mathcal{S} = \{a, b, c\}$, but one can also consider distillation from W states consisting of more than three parties [16]. Although previous studies [14] report a success probability alone, we make the important distinction between

success probability and the expected entanglement. The latter quantity provides a realistic measure of the true utility of a random party distillation protocol for the purpose of entanglement distribution. In subsequent sections, we define our measure $E(\rho_i^k)$ as the entanglement of formation according to [19]. For a pure state $|\psi_{ij}\rangle$, this results in:

$$E(|\psi_{ij}\rangle) = -\text{Tr}\{\rho_i \log_2 \rho_i\} = -\text{Tr}\{\rho_j \log_2 \rho_j\}, \quad (10)$$

where ρ_i corresponds to one subsystem when the other qubit has been traced over:

$$\rho_i = \text{Tr}_j |\psi_{ij}\rangle\langle\psi_{ij}|. \quad (11)$$

For a mixed state ρ , this simply becomes the *minimum* average entanglement of formation over all decompositions of ρ [19]:

$$E(\rho) = \min \sum_k p_k E(|\psi_{ij}^k\rangle\langle\psi_{ij}^k|). \quad (12)$$

At first glance, (12) is an unwieldy calculated calculation; however, it can be greatly simplified by obtaining from a closed-form expression dependent on the Wootters concurrence [19] or bounding with a quantitative witness described in [20].

Replacing the measure $E(\rho_i^k)$ with *distillable entanglement* would indeed be a natural choice, however, we opt to use entanglement of formation for ease of finding an experimental lower bound using either linear witnesses [20] or state fidelity, as will be shown later¹. Furthermore, the entanglement of formation is known to serve as an upper bound to the distillable entanglement [23].

We estimate the EPR distillation rate for up to four rounds of execution by counting the events in which one (and only one) of Alice, Bob, and Charlie measure an outcome of “1” during a round of weak measurements to calculate the success probability given in (8). Fig. 2 shows the probability of success P_N , in which an entangled pair is distilled, and how it experimentally scales with increasing number of rounds. This result is compared to the theoretical prediction in (6). Readout errors are mitigated using a matrix-free measurement error mitigation (M3) approach, as outlined in [15]. Within the first two rounds, the experimental estimation of the protocol’s success rate tracks the theoretical prediction, (6), within $1-\sigma$ error. Importantly, we find that the success

¹ It is possible, however, to obtain a lower bound for distillable entanglement using the entropic uncertainty relations described in [21] or from stabilizer measurements, shown in [22]. These limits have not been proved to be tight.

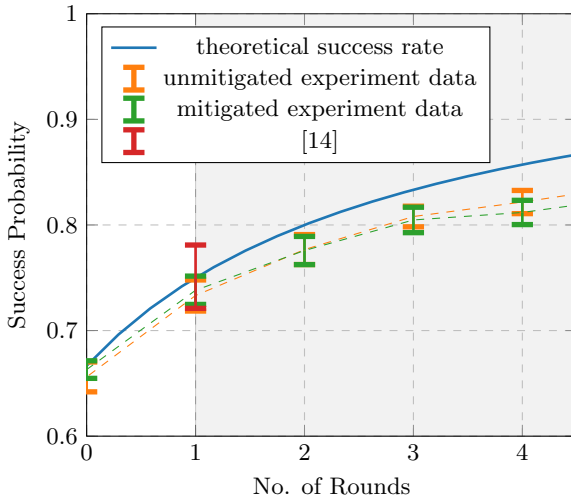


FIG. 2. The probability of successful distillation on `ibm_quebec`. The blue line corresponds to the theoretical prediction, originally derived in [14]. The orange and green data points correspond to unmitigated and mitigated with M3 respectively. Error bars corresponding to $1-\sigma$ uncertainty were obtained by repeating experiments over five consecutive trials. Data outside the shaded grey region were obtained in a *specific* party distillation protocol as opposed to a *random* distillation protocol. We find a record success probability of 81%, superior to both specific party distillation and prior work [14].

probability of our protocol achieves a record rate of 81% for a single copy of a W state, when executing with four rounds of operation. This contrasts with the result of [14], which was limited to a 75% success probability with a chance of false-positive distillation events (indicated by error bars that exceed theoretical limits in distillation rate). The deviation between experiment and theory after the second round can be attributed to a degradation in the fidelity of the W state at the beginning of each round. Furthermore, the estimated rate of success without readout error mitigation will exceed that in which M3 mitigation is employed due to “false-positive” success events from random bit flips in the ancillary qubits.

To confirm the degradation in W state fidelity, we estimate the projector $|W\rangle\langle W|$ after each stage of weak measurements. As shown in (4), the state after coupling to Alice, Bob, and Charlie’s ancillary qubits contains a superposition of both the $|W\rangle$ and $|\Psi^+\rangle$ states. Consequently, one must post-select their measurement results so that instances in which the three parties do not all measure “0” are discarded. Estimation of an observable post-selected on mid-circuit measurement data is a commonplace in quantum computing experiments; all code used in these experiments is provided in [24].

Fig. 3 shows how the fidelity of Alice, Bob, and Charlie’s W state changes at the beginning of each round. We find the most dominant error mechanism to be the

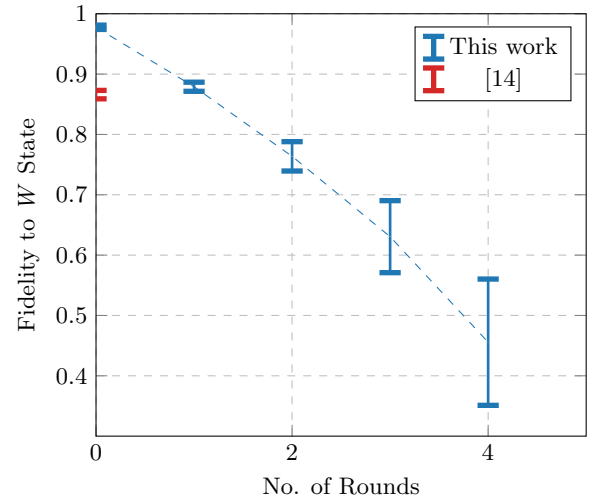


FIG. 3. The evolution of W state fidelity (blue), determined by a series of measurements in the Pauli basis. Error bars corresponding to $1-\sigma$ uncertainty were obtained by repeating experiments over five consecutive trials. The initial W state fidelity of [14] is shown in red for comparison. We find our W state fidelity to exceed that of [14] even after one round of protocol execution.

natural dephasing of qubits on IBM hardware [25]. Dephasing is to be expected in circuits with many stages of mid-circuit measurements, since these often contain idle periods that are relatively long (836 ns) when compared to gate operations (20 - 60 ns). For a deeper discussion on the error mechanisms resulting from mid-circuit measurements in dynamic circuits, the reader is encouraged to consult [26]. We employ XY4 dynamical decoupling [27] on idle qubits during periods of mid-circuit measurements. The XY4 sequence is by no means optimal, since it fails to account for cross-talk between idle qubits; further improvements may require “staggered dynamical decoupling” between neighbouring qubits [28]. Despite the unavoidable degradation in W state fidelity, we find the system to show a better performance than that of [14], where the initial fidelity values are limited to 0.866, versus the value of 0.98 obtained in this work.

Finally, to quantify the performance of our distillation protocol, we estimate a lower bound for the average entanglement of formation of EPR pairs extracted from each stage of protocol execution. To estimate this lower bound, we use a method described by Bennett et al. in [23] that only requires knowledge of the diagonal components of a density matrix in the Bell-basis. We shall refer to this representation as ρ_{BDS} , named after the fact that the state is a “Bell-diagonal state”:

$$\rho_{BDS} = \sum_i \theta_i |\Psi_i\rangle\langle\Psi_i|, \quad (13)$$

where $|\Psi_i\rangle$ refer to the four Bell-states and θ_i are

real-valued weights that sum to one. Intuitively, the weights θ_i also correspond to state fidelities; i.e. $\theta_i = \langle \Psi_i | \rho_{BDS} | \Psi_i \rangle$.

Bennett et al. introduce the largest “fully-entangled fraction” $\theta_{max} = \max_i \theta_i$ as the largest fidelity between a given state and any Bell-state. One can define the function $f(\theta_{max})$:

$$f(\theta_{max}) = \begin{cases} h(1/2 - \sqrt{\theta_{max}(1 - \theta_{max})}) & \theta_{max} > 1/2 \\ 0 & \theta_{max} \leq 1/2 \end{cases}, \quad (14)$$

which is proven in [23] to be a lower bound for the entanglement of formation $E(\rho)$ for *any* spin-1/2 system ρ . The bound reaches equality only when ρ is a Bell-diagonal state. This result implies that with only knowledge of the fidelity to the closest Bell state, one can calculate a lower bound to $E(\rho)$ when $\theta_{max} > 1/2$.

Fig. 4 shows the evolution of both distilled entanglement of formation, and fidelity to the triplet state. All data presented were recorded using an XY4 dynamical decoupling sequence during idle periods. We attribute the non-ideal values of entanglement of formation to the imperfect W states used at the beginning of each round and finite gate errors. Weighting the success probabilities shown in Fig. 2 according to the corresponding entanglement of formation values, we find the average distilled entanglement of our protocol to be as high as $\langle E \rangle \geq 0.5311$ pairs/ W state, when using a single-round implementation of the protocol and as low as $\langle E \rangle \geq 0.4021$ for a four-round implementation. The deterioration in the lower bounds of $\langle E \rangle$ is attributed to a corresponding degradation in the fidelity of the distilled pair (Fig. 4); this is especially damaging to performance, since the probability of success per round decreases as the total number of rounds increases. On the same hardware, we find that the best case of $\langle E \rangle \geq 0.6324$ is obtained by using specific party distillation. The resulting lower bound in expected entanglement shows the advantage of specific party distillation in scenarios where fidelity degrades with circuit depth. Thus, further developments in the performance of the random party distillation rate depend on decoupling from external dephasing channels and having shorter readout periods to minimize errors introduced during mid-circuit measurements.

In this work, we have presented the first physical demonstration of random party distillation that exceeds one round of execution, thus achieving record distillation rate as a result. However, we have also shown how the dephasing of superconducting qubits impacts the quality of both bi- and multipartite entanglement which can be partially mitigated using a combination of dynamical decoupling and M3. More broadly, the results of this work point to the importance of short readout lengths for the execution of either dynamic circuits or those that employ mid-circuit measurements. Such a change would require

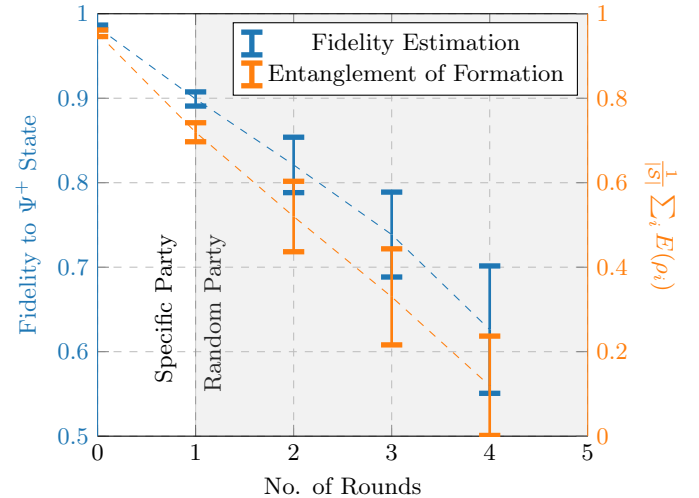


FIG. 4. The evolution of EPR state fidelity and average entanglement of formation (lower bound), measured by a projection onto the Ψ^+ state in the Pauli basis. Error bars corresponding to $1-\sigma$ uncertainty were obtained by repeating experiments over five consecutive trials. Data outside the shaded grey region were obtained in a *specific* party distillation protocol as opposed to a *random* distillation protocol. We observe a deterioration in state fidelity, placing limits on the achievable expected entanglement $\langle E \rangle$.

an entirely new readout architecture, an example being the method of “junction readout” [29]. In the meantime, it is important to explore alternative methods of dynamical decoupling with the goal of preserving multi-qubit entanglement in mind with techniques such as staggered dynamical decoupling [28] and using novel schemes obtained with statistical learning methods [30].

Alternatively, using a device with greater connectivity between qubits would allow the user to use a different set of ancillary qubits with each round of weak measurements. In doing so, one could avoid mid-circuit measurements at the cost of greater overhead in terms of the number of qubits required for bipartite distillation. A presentation of this alternative protocol can be found in the supplementary material to this work in addition to a study of the improvements needed in current hardware necessary for a random party distillation protocol to exceed the expected entanglement $\langle E \rangle$ of the specific party case.

As quantum computing moves toward large-scale distributed architectures [31], the future of random party distillation extends beyond immediate improvements in distillation rates and circuit techniques. Protocols like random party distillation could play an important role in generating high-fidelity entanglement between nodes in a quantum network, a necessary step for enabling robust and fault-tolerant distributed computation [32].

The authors thank Dr. Brian T. Kirby and Dr. Sean

Wagner for insightful discussions. The authors acknowledge the following funding sources: Horizon Europe - Canada Project 101070168 HYPERSPACE, NSERC ALLRP 578462 - 22 and 578460 - 22, CFI and ORF Project 33415, NSERC Discovery Funds RGPIN-2019-07019, RGPAS-2019-00113, and RGPIN-2025-05068. Finally, the authors acknowledge support from the NUS start-up grant.

* alexander.greenwood@mail.utoronto.ca

[1] R. Horodecki, P. Horodecki, M. Horodecki, and K. Horodecki, Quantum entanglement, *Rev. Mod. Phys.* **81**, 865 (2009).

[2] Q.-C. Sun, Y.-F. Jiang, Y.-L. Mao, L.-X. You, W. Zhang, W.-J. Zhang, X. Jiang, T.-Y. Chen, H. Li, Y.-D. Huang, *et al.*, Entanglement swapping over 100 km optical fiber with independent entangled photon-pair sources, *Optica* **4**, 1214 (2017).

[3] E. Bäumer, V. Tripathi, D. S. Wang, P. Rall, E. H. Chen, S. Majumder, A. Seif, and Z. K. Minev, Efficient long-range entanglement using dynamic circuits, *PRX Quantum* **5**, 030339 (2024).

[4] H. Kang, J. F. Kam, G. J. Mooney, and L. C. Hollenberg, Teleporting two-qubit entanglement across 19 qubits on a superconducting quantum computer, *Phys. Rev. Appl.* **23**, 014057 (2025).

[5] B. Fortescue and H.-K. Lo, Random bipartite entanglement from w and w -like states, *Phys. Rev. Lett.* **98**, 260501 (2007).

[6] M. Enríquez, I. Wintrowicz, and K. Życzkowski, Maximally entangled multipartite states: a brief survey, in *Journal of Physics: Conference Series*, Vol. 698 (IOP Publishing, 2016) p. 012003.

[7] J. L. Beckey, N. Gigena, P. J. Coles, and M. Cerezo, Computable and operationally meaningful multipartite entanglement measures, *Phys. Rev. Lett.* **127**, 140501 (2021).

[8] G. Gour, Mixed-state entanglement of assistance and the generalized concurrence, *Phys. Rev. A* **72**, 042318 (2005).

[9] I. Biswas, A. Bhunia, S. Bera, I. Chattopadhyay, and D. Sarkar, Entanglement of assistance as a measure of multiparty entanglement, *Phys. Rev. A* **111**, 032423 (2025).

[10] E. Chitambar, W. Cui, and H.-K. Lo, Entanglement monotones for w -type states, *Phys. Rev. A* **85**, 062316 (2012).

[11] E. Chitambar, W. Cui, and H.-K. Lo, Increasing entanglement monotones by separable operations, *Phys. Rev. Lett.* **108**, 240504 (2012).

[12] G. Liu, I. George, and E. Chitambar, The Round Complexity of Local Operations and Classical Communication (LOCC) in Random-Party Entanglement Distillation, *Quantum* **7**, 1104 (2023).

[13] Y. Wang and E. Chitambar, Random distillation protocols in long baseline telescropy (2024), arXiv:2411.02678 [quant-ph].

[14] Z.-D. Li, X. Yuan, X.-F. Yin, L.-Z. Liu, R. Zhang, Y.-Y. Fei, L. Li, N.-L. Liu, X. Ma, H. Lu, Y.-A. Chen, and J.-W. Pan, Experimental random-party entanglement distillation via weak measurement, *Phys. Rev. Res.* **2**, 023047 (2020).

[15] P. D. Nation, H. Kang, N. Sundaresan, and J. M. Gambetta, Scalable mitigation of measurement errors on quantum computers, *PRX Quantum* **2**, 040326 (2021).

[16] B. Fortescue and H.-K. Lo, Random-party entanglement distillation in multiparty states, *Phys. Rev. A* **78**, 012348 (2008).

[17] W. Cui, E. Chitambar, and H.-K. Lo, Randomly distilling w -class states into general configurations of two-party entanglement, *Phys. Rev. A* **84**, 052301 (2011).

[18] B. Fortescue and H.-K. Lo, Random bipartite entanglement from w and w -like states, *Phys. Rev. Lett.* **98**, 260501 (2007).

[19] W. K. Wootters, Entanglement of formation of an arbitrary state of two qubits, *Phys. Rev. Lett.* **80**, 2245 (1998).

[20] J. Eisert, F. G. Brandao, and K. M. Audenaert, Quantitative entanglement witnesses, *New Journal of Physics* **9**, 46 (2007).

[21] B. Bergh and M. Gärttner, Experimentally accessible bounds on distillable entanglement from entropic uncertainty relations, *Phys. Rev. Lett.* **126**, 190503 (2021).

[22] H.-K. Lo, Proof of unconditional security of six-state quantum key distribution scheme, *Quantum Information & Computation* **1**, 81 (2001).

[23] C. H. Bennett, D. P. DiVincenzo, J. A. Smolin, and W. K. Wootters, Mixed-state entanglement and quantum error correction, *Phys. Rev. A* **54**, 3824 (1996).

[24] A. Greenwood and J. Russett, Conditional Measurement Toolbox (2025).

[25] A. Rahman, D. J. Egger, and C. Arenz, Learning how to dynamically decouple by optimizing rotational gates, *Phys. Rev. Appl.* **22**, 054074 (2024).

[26] L. Shirizly, L. C. G. Govia, and D. C. McKay, Randomized benchmarking protocol for dynamic circuits, *Phys. Rev. A* **111**, 012611 (2025).

[27] N. Ezzell, B. Pokharel, L. Tewala, G. Quiroz, and D. A. Lidar, Dynamical decoupling for superconducting qubits: A performance survey, *Physical Review Applied* **20**, 064027 (2023).

[28] S. Niu, A. Todri-Sanial, and N. T. Bronn, Multi-qubit dynamical decoupling for enhanced crosstalk suppression, *Quantum Science and Technology* **9**, 045003 (2024).

[29] A. A. Chapple, O. Benhayoune-Khadraoui, S. Richer, and A. Blais, Balanced cross-kerr coupling for superconducting qubit readout (2025), arXiv:2501.09010 [quant-ph].

[30] C. Tong, H. Zhang, and B. Pokharel, Empirical learning of dynamical decoupling on quantum processors (2025), arXiv:2403.02294 [quant-ph].

[31] M. Mohseni, A. Scherer, K. G. Johnson, O. Wertheim, M. Otten, N. A. Audit, Y. Alexeev, K. M. Bresnicker, K. Y. Camsari, B. Chapman, S. Chatterjee, G. A. Dagnaw, A. Esposito, F. Fahim, M. Fiorentino, A. Gajjar, A. Khalid, X. Kong, B. Kulchytskyy, E. Kyoseva, R. Li, P. A. Lott, I. L. Markov, R. F. McDermott, G. Pedretti, P. Rao, E. Rieffel, A. Silva, J. Sorebo, P. Spentzouris, Z. Steiner, B. Torosov, D. Venturelli, R. J. Visser, Z. Webb, X. Zhan, Y. Cohen, P. Ronagh, A. Ho, R. G. Beausoleil, and J. M. Martinis, How to build a quantum supercomputer: Scaling from hundreds to millions of qubits (2025), arXiv:2411.10406 [quant-ph].

[32] A. Carrera Vazquez, C. Tornow, D. Ristè, S. Woerner, M. Takita, and D. J. Egger, Combining quantum proces-

sors with real-time classical communication, *Nature* , 1 (2024).

Supplementary Information: Random Party Distillation on a Superconducting Quantum Processor

I. SYSTEM BENCHMARKING

In what follows, we present basic properties of the superconducting processor used for all experiments (`ibm_quebec`) including generated W state fidelity, and properties of the qubits themselves taken at the time of data collection. The efficacy of the protocol depends on the fidelity of W -state used in each round of execution.

Fig. 1 shows the density matrix measured before protocol execution (after W state initialization) with a three-qubit quantum state tomography. Inevitable readout errors are calibrated by assuming tensor product and correlated Markovian noise models, as presented in [1]. Inevitable readout errors are calibrated by assuming a “tensor product noise model” defined according to [1, 2]. With such a model, we assume that readout errors are primarily uncorrelated, i.e. little crosstalk between qubits during measurement, and measurement outcomes may be mapped to their corrected values with a “mitigation matrix” obtained from an initial calibration procedure defined in [2]. We estimate the fidelity to the ideal W state, to be 0.958 ± 0.007 ($1-\sigma$ error) by measuring the projector $|W\rangle\langle W|$ over 1000 shots.

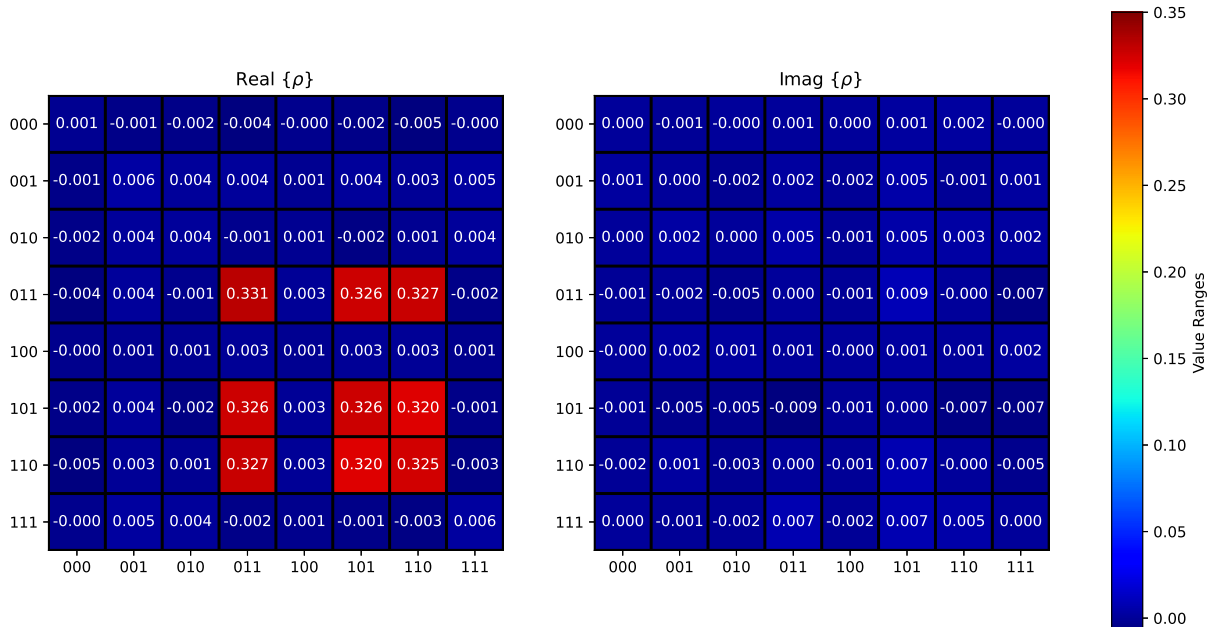


FIG. 1. The density matrix of a W state created on `ibm_quebec`. The fidelity to the ideal scenario is found to be 0.958 ± 0.007 ($1-\sigma$ error).

All relevant properties of the qubits used in this work are outlined in Table I.

Qubit	Physical Qubit	Coherence Time T_1 (μ s)	Dephasing Time T_2 (μ s)	Readout Error	Readout length (ns)
a	23	366.1082	216.9724	0.0100	835.5556
b	24	382.6895	182.1576	0.0283	835.5556
c	25	306.8350	482.8157	0.0066	835.5556
α	22	371.1372	288.1581	0.0244	835.5556
β	34	282.4133	163.5965	0.0310	835.5556
γ	26	399.3776	414.6890	0.0259	835.5556

TABLE I. Physical parameters pertinent to the experiments presented in the manuscript. All parameters were taken from the superconducting device, `ibm_quebec`.

II. MEASURING CONDITIONAL OBSERVABLES

All probabilities of successful distillation and lower bounds for entanglement of formation used to calculate the expected entanglement $\langle E \rangle$ can be found in tables II - V and ?? - VI, respectively.

Round	P(W)	P(EPR) (weak measurement)	P(EPR) (strong measurement)
0	-	-	0
1	0.4113	0.3446	0.3936

TABLE II. The estimated probabilities corresponding to a W state and EPR pair being extracted from round i for a single round protocol (with strong measurement). The estimated entanglement $\langle E \rangle$ is calculated to be $\langle E \rangle \geq 0.5311$.

Round	P(W)	P(EPR) (weak measurement)	P(EPR) (strong measurement)
0	-	-	0
1	0.5472	0.2842	0
2	0.2493	0.2123	0.2792

TABLE III. The estimated probabilities corresponding to a W state and EPR pair being extracted from round i for a two-round protocol (with strong measurement). The estimated entanglement $\langle E \rangle$ is calculated to be $\langle E \rangle \geq 0.4601$.

Round	P(W)	P(EPR) (weak measurement)	P(EPR) (strong measurement)
0	-	-	0
1	0.5927	0.3115	0
2	0.3208	0.1876	0
3	0.1477	0.1406	0.1651

TABLE IV. The estimated probabilities corresponding to a W state and EPR pair being extracted from round i for a three-round protocol (with strong measurement). The estimated entanglement $\langle E \rangle$ is calculated to be $\langle E \rangle \geq 0.4225$.

Round	P(W)	P(EPR) (weak measurement)	P(EPR) (strong measurement)
0	-	-	0
1	0.6381	0.2499	0
2	0.3830	0.1942	0
3	0.2101	0.1358	0
4	0.1020	0.0989	0.1331

TABLE V. The estimated probabilities corresponding to a W state and EPR pair being extracted from round i for a four-round protocol (with strong measurement). The estimated entanglement $\langle E \rangle$ is calculated to be $\langle E \rangle \geq 0.3533$.

Round	$\frac{1}{ S } \sum_i E(\rho_i^k), \frac{1}{ S } \sum_i E(\rho_i^s)$
0	0.9538 ± 0.0078
1	0.7195 ± 0.0225
2	0.52 ± 0.0834
3	0.3298 ± 0.1137
4	0.1193 ± 0.1176

TABLE VI. The estimated lower bounds in entanglement of formation $E(\rho_j)$ for each EPR pair extracted by Alice at round i by process of *weak measurement*. For simplicity, we have assumed that this is equal to the average distilled entanglement of the state after a successful *strong*

III. RANDOM PARTY DISTILLATION WITHOUT MIDCIRCUIT MEASUREMENTS

In the main text, we point out that the dominant source of error in our random party distillation experiments arises from mid-circuit measurements. Recent texts on mid-circuit measurements, notably [3] and [4], point to both

dephasing and crosstalk as nearly unavoidable even with current dynamical decoupling techniques. In this section, we propose an alternative form of Random Party Distillation, making use of no mid-circuit measurements, at the cost of requiring a larger number of ancillary qubits.

The revised version of the protocol takes a form similar to that proposed in the main text. Alice, Bob, and Charlie prepare a state $|W\rangle$ of the form

$$|W\rangle = \frac{1}{\sqrt{3}} (|011\rangle + |101\rangle + |110\rangle). \quad (1)$$

Each “round” of the protocol once again consists of Alice, Bob, and Charlie weakly measuring their respective qubits. “Weak measurements” in our case consist of weakly coupling an ancillary qubit (probe) to a qubit belonging to the original W state (system) using a $CRY(\theta)$ gate. Once again, we define the $CRY(\theta)$ gate:

$$\begin{aligned} CRY(\theta)_{A_i,i} &= \mathbb{1} \otimes |0\rangle\langle 0| + RY(\theta) \otimes |1\rangle\langle 1| \\ &= \begin{bmatrix} 1 & 0 & 0 & 0 \\ 0 & \cos\left(\frac{\theta}{2}\right) & 0 & -\sin\left(\frac{\theta}{2}\right) \\ 0 & 0 & 1 & 0 \\ 0 & \sin\left(\frac{\theta}{2}\right) & 0 & \cos\left(\frac{\theta}{2}\right) \end{bmatrix}. \end{aligned} \quad (2)$$

Once again, the choice of θ_D is related to the measurement strength ϵ_D by the following formula:

$$\theta_D = 2 \arcsin(\epsilon_D). \quad (3)$$

The measurement strength ϵ_D depends on the number of remaining rounds D and is given by

$$\epsilon_D = \frac{1}{\sqrt{D+5}}. \quad (4)$$

Previously, this would have been followed by Alice, Bob, and Charlie performing projective (mid-circuit) measurements defined by the operators $F = |0\rangle_{A_i} \langle 0|_{A_i}$ and $G = |1\rangle_{A_i} \langle 1|_{A_i}$. In this revised version of the protocol, the three parties instead perform a series of cascaded CNOT operations between ancillary qubits. In operator form, Alice, Bob, and Charlie perform the following operation:

$$\prod_i^D U_{CNOT}^{k(D-i)(D-i+1)} \rho_{wm} \prod_i^D \left(U_{CNOT}^{k(D-i)(D-i+1)} \right)^\dagger, \quad (5)$$

where U_{CNOT}^{kij} represent the CNOT gates performed by the k th party (Alice, Bob, or Charlie) between qubits i and j :

$$U_{CNOT}^{kij} = |0\rangle\langle 0|_{ki} \otimes |0\rangle\langle 0|_{kj} + |1\rangle\langle 1|_{ki} \otimes |1\rangle\langle 1|_{kj} + |1\rangle\langle 1|_{ki} \otimes |0\rangle\langle 1|_{kj} + |0\rangle\langle 0|_{ki} \otimes |1\rangle\langle 1|_{kj}. \quad (6)$$

The state ρ_{wm} represents the W state possessed by the three parties, *after* having performed the controlled rotations $CRY(\theta)$:

$$\rho_{wm} = CRY(\theta)_{\alpha 1,a} CRY(\theta)_{\beta 1,b} CRY(\theta)_{\gamma 1,c} |W\rangle\langle W| CRY(\theta)_{\alpha 1,a}^\dagger CRY(\theta)_{\beta 1,b}^\dagger CRY(\theta)_{\gamma 1,c}^\dagger, \quad (7)$$

where we have assumed that the ancillary qubits $(\alpha_1, \beta_1, \gamma_1)$ are initialized in the ground state. Fig. 2 shows a circuit diagram and connectivity graph of the proposed protocol.

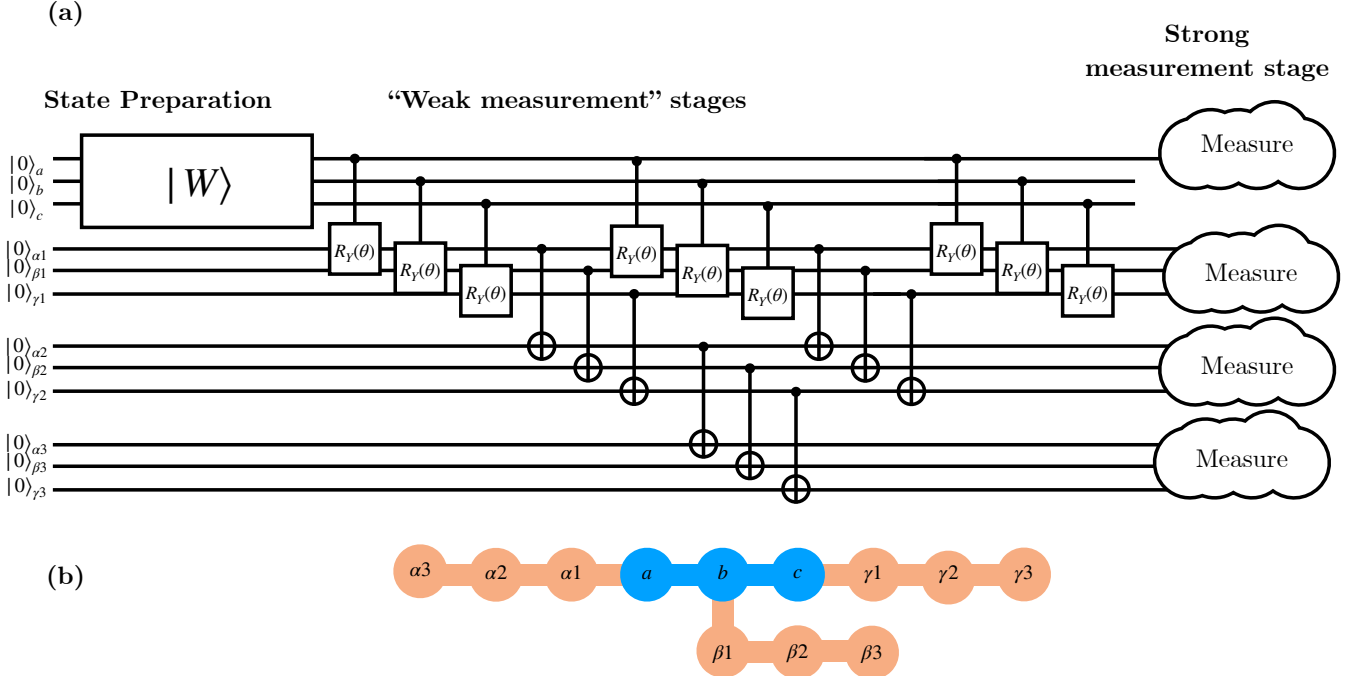


FIG. 2. (a) A circuit diagram showing our proposed random party distillation protocol *without* need for mid-circuit measurements. (b) The corresponding qubit connectivity graph showing signal qubits (blue) and ancillae (orange). Mid-circuit measurements are replaced with an additional step where information carried by qubits (i.e. weak measurement outcomes) is transferred to nearest, next-nearest, etc. neighbours so that $\alpha_1, \beta_1, \gamma_1$ may be reused for subsequent rounds.

Following this proposal, we demonstrated the protocol's performance on the 156 qubit Heron r2 processor, `ibm_fez`. The evolution in distilled pair fidelity for both the protocol with and without mid-circuit measurements is shown in Fig. 3. Similar to the experiments presented in the body-text, XY4 dynamical decoupling sequences were used, followed by M3 for measurement-error mitigation.

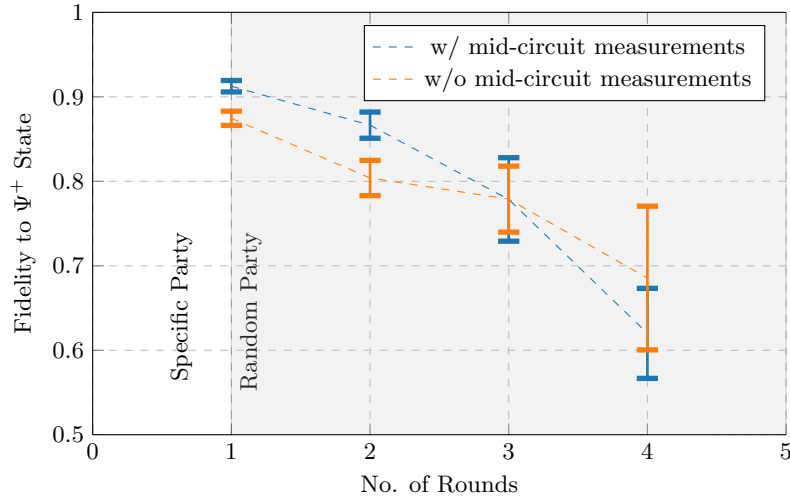


FIG. 3. The evolution of EPR state fidelity, measured by a projection onto the Ψ^+ state in the Pauli basis. Error bars corresponding to $1-\sigma$ uncertainty were obtained by repeating experiments over five consecutive trials.

As shown in Fig. 3, we find that the state of the system after a successful distillation event has fidelity comparable to the EPR state, regardless of whether or not mid-circuit measurements are used. The resulting fidelity is unsurprising,

considering the number of CNOT operations required for protocol execution, introducing both gate error (median 2.73×10^{-3}) and cumulative gate durations comparable to the process of mid-circuit measurement (68 ns/ECR operation). Much like our protocol requiring mid-circuit measurements, we predict that further improvements will arise from shorter gate operations to prevent dephasing from the external environment.

IV. SIMULATING NOISY RANDOM PARTY DISTILLATION

In what follows, we shall consider the simulation of a random party distillation protocol using noisy qubits, and imperfect gate operations.

We shall treat our imperfect W state in all stages of the random party distillation experiment as a convex combination of the following form:

$$W_{\text{imp}} = (1 - p) |W\rangle\langle W| + \frac{p}{8} \mathbb{1}, \quad (8)$$

where $|W\rangle$ is the familiar W state:

$$|W\rangle = \frac{1}{\sqrt{3}} (|110\rangle + |101\rangle + |011\rangle). \quad (9)$$

We shall consider the expected entanglement $\langle E \rangle$ defined in the main text for a single round of random party distillation when starting with an imperfect W state while using perfect gate operations. Once again, we assume that our initial state is of the form (8) with a fidelity of 0.97 (as quoted in the main text). Following the protocol proposed in the main text, the first weak measurement stage consists of a controlled RY operation between Alice, Bob, and Charlie's qubits (where their 'signal' qubit is the control and their ancilla is target). The probability of success can be obtained by simply estimating the expectation values of the projectors $\text{Per}\{F \otimes F \otimes G\}$ where $F = |0\rangle_{A_i}\langle 0|_{A_i}$ and $G = |1\rangle_{A_i}\langle 1|_{A_i}$ and $\text{Per}\{\cdot\}$ represents all permutations of argument operators. Similarly, one can extract the corresponding mixed state entanglement of formation by calculating the Wootters concurrence $\mathcal{C}(\rho)$ [5] of the state ρ_i remaining from tracing over party i after a round of weak measurements. That is,

$$\mathcal{C}(\rho) = \max\{0, \lambda_1 - \lambda_2 - \lambda_3\}, \quad (10)$$

where λ_i s are the eigenvalues (in decreasing order) of the Hermitian matrix R

$$R = \sqrt{\sqrt{\rho} \tilde{\rho} \sqrt{\rho}} \quad (11)$$

and

$$\tilde{\rho} = (\sigma_y \otimes \sigma_y) \rho^* (\sigma_y \otimes \sigma_y). \quad (12)$$

Finally, we use the well-known formula for entanglement of formation E :

$$E(\mathcal{C}) = h(1/2 - \sqrt{1 - \mathcal{C}^2}), \quad (13)$$

where $h(\cdot)$ is the binary entropy function (described in the main text).

Afterwards, we start with a state of the form (8) of lower fidelity, to simulate the effects of dephasing on the superconducting processor. We repeat the aforementioned process of weak measurements for as many rounds as required in the protocol, adjusting the state fidelity with each round. After the weak measurement stages have completed, we perform a final round of specific party distillation. Fig. 4 summarizes the aforementioned process used for simulation.

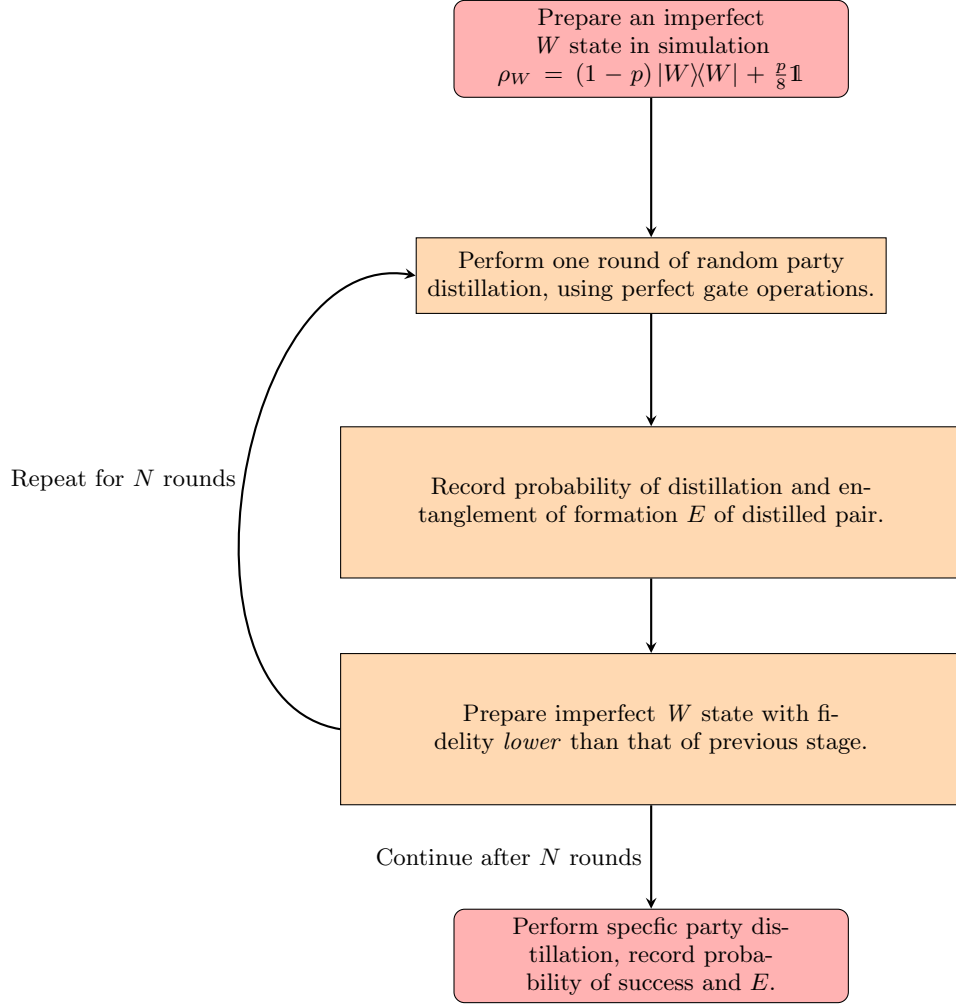


FIG. 4. A flow-chart depicting the process by which the success rate of a one-way distillation protocol is obtained from estimating the expectation values of Pauli observables.

As an example, we simulate the protocol's performance for a single round of random party distillation followed by specific party distillation. Fig. 5 displays the expected entanglement $\langle E \rangle$ obtained from a single round of random party distillation for fidelity values (in the range $F \in [0, 0.97]$) of the noisy W state after the first round of weak measurements.

As expected, we find that an improvement in $\langle E \rangle$ occurs when the fidelity of the noisy W state exceeds 0.95. Furthermore, we find the model's prediction of $\langle E \rangle \approx 0.555$ for a first-round fidelity of $F \approx 0.9$ tracks our experimental results with high accuracy (within 4.3%).

Indeed, the close agreement between our simplistic model using perfect gate operations and experiment supports the claim that mid-circuit measurements are the dominant source of error in our systems (rather than gate errors).

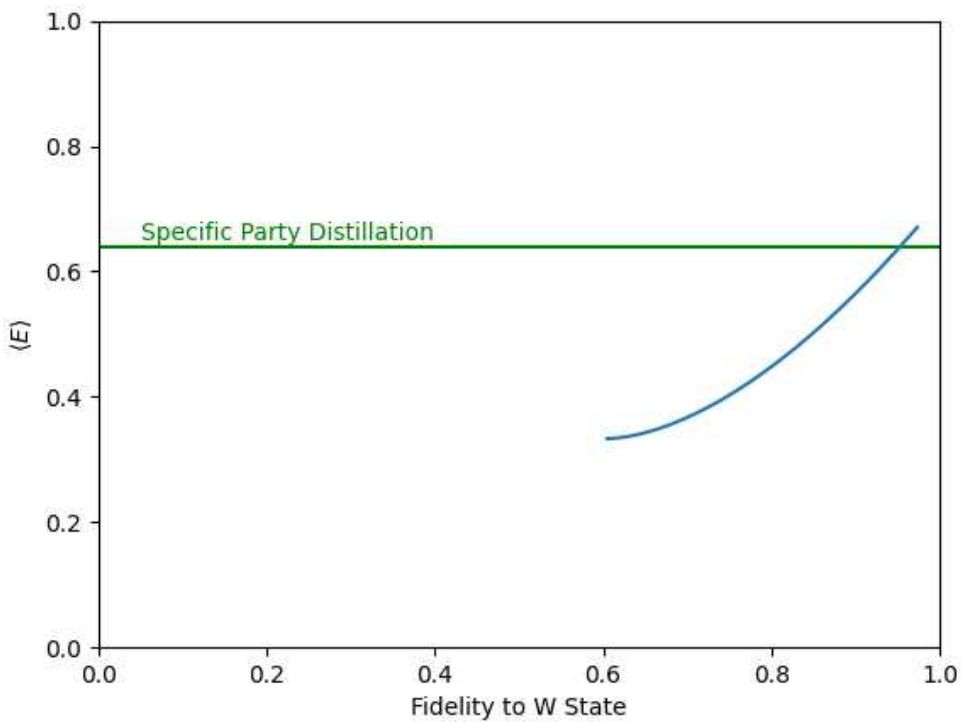


FIG. 5. The Fidelity of a noisy W state ρ_W to the ideal W state *after* 1 round of random party distillation (blue) when compared against specific party distillation (green) starting with fidelity of 0.97.

[1] S. Bravyi, S. Sheldon, A. Kandala, D. C. Mckay, and J. M. Gambetta, Mitigating measurement errors in multiqubit experiments, *Phys. Rev. A* **103**, 042605 (2021).

[2] N. Kanazawa, D. J. Egger, Y. Ben-Haim, H. Zhang, W. E. Shanks, G. Aleksandrowicz, and C. J. Wood, Qiskit Experiments: A Python package to characterize and calibrate quantum computers, *Journal of Open Source Software* **8**, 5329 (2023).

[3] D. Hothem, J. Hines, C. Baldwin, D. Gresh, R. Blume-Kohout, and T. Proctor, Measuring error rates of mid-circuit measurements, *Nature Communications* **16**, 5761 (2025).

[4] L. Shirizly, L. C. G. Govia, and D. C. McKay, Randomized benchmarking protocol for dynamic circuits, *Phys. Rev. A* **111**, 012611 (2025).

[5] W. K. Wootters, Entanglement of formation of an arbitrary state of two qubits, *Phys. Rev. Lett.* **80**, 2245 (1998).